Presenilin 1 Deficiency Alters the Activity of Voltage-Gated Ca^{2+} Channels in Cultured Cortical Neurons

David G. Cook,[1,2] Xiaofan Li,[3] Sheree D. Cherry,[3] and Angela R. Cantrell[3]

[1]*Veterans Affairs Puget Sound Health Care System, Geriatric Research Education and Clinical Center (GRECC), Seattle, Washington;*
[2]*Division of Gerontology and Geriatric Medicine, Department of Medicine, University of Washington School of Medicine, Seattle Washington; and* [3]*Department of Anatomy and Neurobiology, University of Tennessee Health Science Center, Memphis Tennessee*

Cook, David G., Xiaofan Li, Sheree D. Cherry, and Angela R. Cantrell. Presenilin 1 deficiency alters the activity of voltage-gated Ca^{2+} channels in cultured cortical neurons. *J Neurophysiol* 94: 4421–4429, 2005. First published September 7, 2005; doi:10.1152/jn.00745.2005. Presenilins 1 and 2 (PS1 and PS2, respectively) play a critical role in mediating γ-secretase cleavage of the amyloid precursor protein (APP). Numerous mutations in the presenilins are known to cause early-onset familial Alzheimer's disease (FAD). In addition, it is well established that PS1 deficiency leads to altered intracellular Ca^{2+} homeostasis involving endoplasmic reticulum Ca^{2+} stores. However, there has been little evidence suggesting Ca^{2+} signals from extracellular sources are influenced by PS1. Here we report that the Ca^{2+} currents carried by voltage-dependent Ca^{2+} channels are increased in PS1-deficient cortical neurons. This increase is mediated by a significant increase in the contributions of L- and P-type Ca^{2+} channels to the total voltage-mediated Ca^{2+} conductance in PS1 ($-/-$) neurons. In addition, chelating intracellular Ca^{2+} with 1,2-bis-(o-aminophenoxy)ethane-*N,N,N′,N′*-tetraacetic acid (BAPTA) produced an increase in Ca^{2+} current amplitude that was comparable to the increase caused by PS1 deficiency. In contrast to this, BAPTA had no effect on voltage-dependent Ca^{2+} conductances in PS1-deficient neurons. These data suggest that PS1 deficiency may influence voltage-gated Ca^{2+} channel function by means that involve intracellular Ca^{2+} signaling. These findings reveal that PS1 functions at multiple levels to regulate and stabilize intracellular Ca^{2+} levels that ultimately control neuronal firing behavior and influence synaptic transmission.

INTRODUCTION

Presenilin 1 and 2 (PS1 and PS2, respectively) are ubiquitously expressed polytopic membrane-spanning proteins that are best appreciated for their role in regulating cleavage of the amyloid precursor protein (APP) to produce the Alzheimer's disease related peptide, A-beta (Aβ) (Doan et al. 1996; Haass 1997; Li and Greenwald 1996). Early onset familial Alzheimer's disease (FAD) is associated with >100 presenilin mutations, the vast majority of which occur in PS1 (Levy-Lahad et al. 1995; Rogaev et al. 1995; Selkoe 1997; Sherrington et al. 1995). PS1 also regulates cleavage of Notch (Baumeister et al. 1997; Levitan et al. 1996; Struhl and Greenwald 1999), Delta1 and Jagged2 (Ikeuchi and Sisodia 2003), ErbB-4 (Ni et al. 2001), E-cadherin (Marambaud et al. 2002), LDL receptor-related protein (May et al. 2002), and Na$^+$ channel β subunits (Kim et al. 2005; Wong et al. 2005); and regulates protein trafficking (Cai et al. 2002; Leem et al. 2002; Naruse et al.

1998), apoptosis (Mattson et al. 1998; Wolozin et al. 1998), and experience-dependent neurogenesis (Feng et al. 2001). In addition, several laboratories have reported that PS1 plays an important role in regulating intracellular Ca^{2+} homeostasis involving endoplasmic reticulum Ca^{2+} stores (Begley et al. 1999; Guo et al. 1999a; Herms et al. 2003; Ito et al. 1994; Leissring et al. 1999a,b; Stutzmann et al. 2004; Yoo et al. 2000). PS1-deficiency ($-/-$) significantly impairs intracellular Ca^{2+} homeostasis (Leissring et al. 2002; Yang and Cook 2004; Yoo et al. 2000). This defect is attributable to reduced levels of Ca^{2+} release from inositol 1,4,5-trisphosphate (IP$_3$)-sensitive intracellular stores (LaFerla 2002; Leissring et al. 1999b, 2000, 2002).

A great deal of effort has been expended to further characterize and understand the role of PS1 in regulating intracellular Ca^{2+} homeostasis and much has been learned. However, there is currently little evidence to suggest that PS1 also influences Ca^{2+} homeostasis via plasma membrane Ca^{2+} channels. Therefore the goal of the present work was to examine whether the alterations in Ca^{2+} homeostasis in PS 1-deficient mice include any changes in the voltage-dependent Ca^{2+} current carried by plasma membrane channels. Using primary cultured cortical neurons derived from PS1 wild-type ($+/+$) and PS1 knock-out ($-/-$) mice (Shen et al. 1997), we found that PS1-deficiency increased the total voltage-mediated Ca^{2+} conductance via L- and P-type Ca^{2+} channels. The effect of PS1-deficiency on voltage-gated Ca^{2+} currents was mimicked in wild-type neurons following experimental manipulations designed to reduce intracellular Ca^{2+} signals. Peak Ca^{2+} current amplitude was increased in wild-type neurons dialyzed with 10 mM 1,2-bis-(o-aminophenoxy)ethane-*N,N,N′,N′*-tetraacetic acid (BAPTA) or treated chronically with caffeine to levels similar to those observed in PS1-deficient neurons. There was no discernable affect of these experimental manipulations in PS1-deficient neurons whose intracellular Ca^{2+} signals are already reduced. These data suggest an interaction between voltage-gated Ca^{2+} channel function and the depletion of intracellular Ca^{2+} stores caused by PS1 loss of function. These are the first data showing that PS1 influences Ca^{2+} homeostasis via voltage-gated Ca^{2+} channels. These results must be taken into consideration when attempting to explain the role of PS1 in regulating and stabilizing intracellular Ca^{2+} levels and ultimately in regulating synaptic transmission.

Address for reprint requests and other correspondence: A. R. Cantrell, Dept. of Anatomy and Neurobiology, University of Tennessee Health Science Center, 855 Monroe Ave., Link 515, Memphis, TN 38163 (E-mail: acantrell@utmem.edu).

METHODS

Generation of PS1-deficient mice

Embryonic mice derived from PS1 doubly heterozygous (+/−) crosses were genotyped using three PCR primers (primer 1: 5′-ACCTCAGCTGTTTGTCCCGG-3′, primer 2: 5′-GCACGAGACT-AGTGAGACGTG-3′, and primer 3: 5′-CTGGAAGTAG-GACA-AAGGTG-3′). Primers 1 and 3 generated a 345-base pair (bp) PCR product diagnostic of a wild-type genotype, whereas primers 1 and 2 yielded a 300-bp band indicating a knock-out genotype (Shen et al. 1997). Experiments were performed using PS1 (−/−) mice back-crossed into a C57BL6 genetic background >10 generations.

Primary neuronal culture

These experiments were performed using age-matched cortical neurons from embryonic mice maintained in primary culture. All animal protocols were reviewed and approved by the institutional IACUC committees at the University of Tennessee Health Science Center and the University of Washington VAPSHCS. Cortical tissue was obtained from PS1-deficient (−/−), PS1-wild-type (+/+) and PS1-heterozygous (+/−) mouse embryos on days E15–E21 and stored in hibernation media (Gibco BRL; Rockville, MD) at 4°C for <24 h prior to use. Prior to plating, the tissue was transferred to a 15 ml conical tube containing 1 ml Ca^{2+}-, Mg^{2+}-free Hank's basic salt solution (HBSS; pH = 7.37; Gibco BRL) supplemented with 10 mM HEPES (Sigma; St. Louis, MO) and 1 mM pyruvate (Sigma). The tissue was then dissociated using a fire-polished Pasteur pipette. Following trituration, 2 ml Ca^{2+}-, Mg^{2+}-containing HBSS was added to the tube, and the tissue was allowed to settle for 3 min. The supernatant was then transferred to two 1.5-ml microcentrifuge tubes and spun at 8,800 rpm to pellet the cortical neurons. The cells were then resuspended in 3 ml Neurobasal Media (Gibco BRL) supplemented with B-27 (1:50; Gibco BRL), glutamine (0.5 mM; Sigma), glutamate (25 μM; Sigma), and PenStrep (100 U/ml; Sigma) and plated onto poly-D-lysine (Sigma) treated 35-mm plastic tissue culture dishes at a density of 100,000–200,000 cells per dish. Plates were incubated at 37°C, 5% CO_2 until recording. The cultures were fed every 4 days with Neurobasal Media supplemented with B-27 (1:50), glutamine (0.5 mM) and PenStrep (100 U/ml). Neurons were studied after being maintained in culture for 10–12 days to allow time for the normal developmental upregulation of voltage-gated Ca^{2+} channels (Foehring and Lorenzon 1999; Lorenzon and Foehring 1995).

Whole cell (WC) recordings

Standard WC voltage-clamp recording techniques were employed to record WC Ca^{2+} current from visually identified cortical neurons with pyramidal morphology and relatively short processes (Surmeier et al. 1992). The external recording solution consisted of (in mM) 20 NaCl, 10 HEPES, 4 $MgCl_2$, 50 CsCl, 10 $BaCl_2$, 80 glucose, and 0.001 tetrodotoxin (TTX) (pH = 7.3, 300–310 mOsm/L; all components obtained from Sigma). The internal recording solution consisted of (in mM) 189 N-methyl D-glucamine, 40 HEPES, 1 NaCl, 0.1 BAPTA, 25 phosphocreatine, 2–4 Na_2ATP, 0.2 Na_3GTP, and 0.1 leupeptin (pH = 7.3, 270–280 mOsm/L; all components obtained from Sigma except BAPTA obtained from Calbiochem; San Diego, CA). BAPTA (10 mM) was added to the internal solution where indicated. This solution was allowed to dialyze into the neuron for ≥5 min prior to beginning the experiment. The inclusion of TTX (Sigma) to block Na^+ channels and Cs^+ to block K^+ channels ensured that the voltage-gated Ca^{2+} current was recorded in isolation. Because Cs^+ blocks many but not all K^+ channels, we assessed the sensitivity of the remaining current to block by Cd^{2+}. The remaining current in these cells was completely blocked by 200 μM Cd^{2+}, indicating that the current under study was mediated by voltage-gated Ca^{2+} channels. Electrodes were pulled from micropipette glass and fire-polished prior to use. Electrode

resistances were normally 3–6 MΩ, and final series resistance values averaged 6-8MΩ. Series resistance compensation (80%) was routinely employed. Recordings were obtained using an Axon Instruments 200B patch clamp. Voltage pulses were delivered and currents were recorded using a personal computer running pClamp software to control AD/DA interface. Drugs were applied using a motor-driven "sewer pipe" system that allowed rapid solution changes. The perfusion array was located a few hundred micrometers away from the cell under study. Concentrated stocks of caffeine (Sigma), ω-conotoxin GVIA (Alomone; Jerusalem, Israel), ω-agatoxin IVA (Alomone), ω-conotoxin MVIIC (Alomone), and TTX were made in water, aliquoted and frozen until use. When using ω-agatoxin IVA, cytochrome C (Calbiochem) was added to all solutions (0.01%) to prevent nonspecific binding to plastics. Concentrated stocks of nifedipine (Sigma RBI) were made in 100% ethanol, aliquoted and frozen prior to use. Ethanol and cytochrome C vehicle controls were performed where necessary.

Data analysis

Data were collected using standard voltage step or voltage ramp protocols. WC currents were elicited by a series of 300-ms depolarizing test pulses in the range of −70 to 50 mV from a holding potential of −110. Conductance (g) was calculated from peak current where $g(V) = I(V − V_{rev})$, where I was the current, V was the test pulse voltage, and V_{rev} was the measured reversal potential. Conductance-voltage curves were fit with a Boltzmann function of the form: $g(V) = g_{max}/\{1 + \exp[(V − V.5)/k]\}$, where $V.5$ was the half activation voltage, k was the slope factor and g_{max} was the maximum conductance. Least-squares curve fitting and statistical analysis were done using Sigma Plot (SPSS, Chicago, IL) and Origin (Microcal, Northampton, MA). Statistics are presented as means ± SE. Statistical significance was established by Student's t-test or one-way ANOVA followed by post hoc Sheffé's analysis with P values as reported.

RESULTS

We examined the physiological properties of the WC high-voltage activated (HVA) Ca^{2+} current in PS1-wild-type (+/+), PS1-heterozygous (+/−), and PS1-deficient (−/−) cortical neurons at DIV 10–12. WC current was elicited by a series of depolarizing test pulses in the range of −70 to +50 mV from a holding potential of −110 mV (Fig. 1, A and B). In most cells, the current was exclusively of the HVA type. Only infrequently did we see evidence of low-voltage activated (LVA) currents. Under our normal recording conditions, in the presence of TTX to block voltage-gated Na^+ current and Cs^+ to block voltage-gated K^+ current, the remaining current was completely blocked by 200 μM Cd^{2+} (data not shown), indicating that the current under study was mediated by voltage-gated Ca^{2+} channels. We found that the peak HVA Ca^{2+} current amplitude was significantly different across the three groups (one-way ANOVA, $P = 0.00006$). Post hoc comparison using Sheffé's analysis indicated that peak HVA Ca^{2+} current amplitude was significantly increased in the PS1-deficient neurons (Fig. 1, A–D). Peak current amplitude for PS1 (+/+) cortical neurons was 268.7 ± 16.3 pA ($n = 71$) compared with 438.7 ± 31.1 pA ($n = 94$; $P < 0.005$, Scheffé's test) for PS1 (−/−) cortical neurons. The PS1 (+/−) neurons had an intermediate peak current amplitude (405.3 ± 46.4 pA; $n = 28$) suggesting a gene dosage effect of PS1.

One possible explanation for this observation is that the increase in peak current amplitude was due to increased cell size in the PS1 (−/−) neurons. To rule out this possibility, we
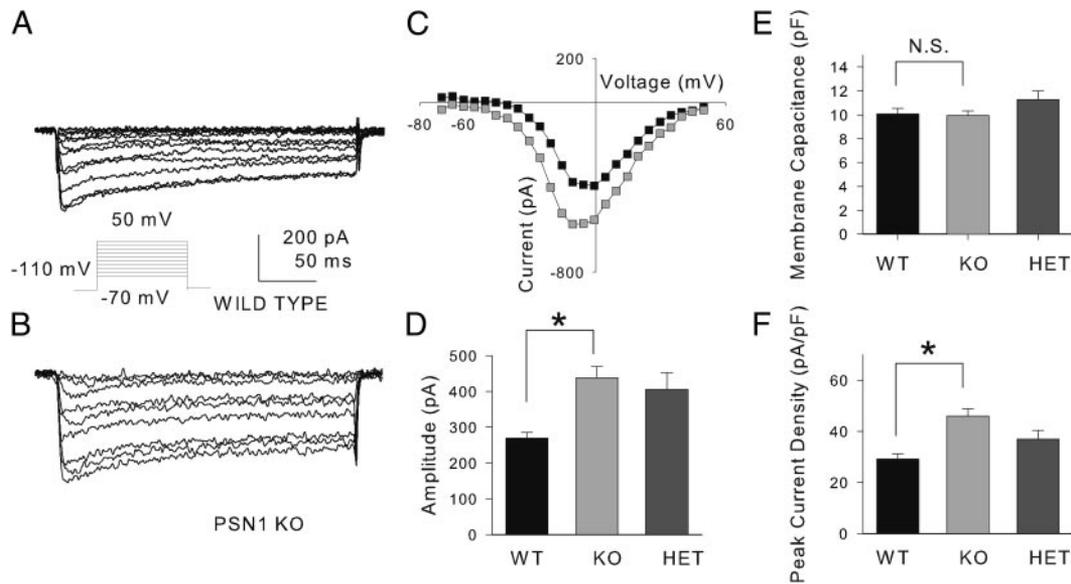
FIG. 1. High-voltage activated (HVA) Ca^{2+} currents are increased in cortical neurons from presenilin 1 (PS1)-deficient mice. A and B: whole cell Ca^{2+} (+/−) current was elicited by a series of depolarizing steps from −70 to 50 mV (250 ms) from a holding potential of −110 mV in PS1 wild-type (WT) (+/+) and PS1 (−/−) cortical neurons. C: plot of peak current vs. voltage for the data shown in A (■) and B (□). D–F: bar graphs depicting statistical summaries of peak current amplitude (D), membrane capacitance (E), and peak current density (F) for populations of PS1 WT (+/+) (n = 71), PS1 heterozygous (+/−) (n = 28) and PS1 (−/−) (n = 94) neurons. Error bars depict SE. *, statistically significant differences of P < 0.005 as determined by one-way ANOVA followed by post hoc Scheffé's analysis. NS, indicates statistical nonsignificance.

assessed cell size using membrane capacitance measures. Membrane capacitance is defined as the amount of charge across the membrane bilayer and is therefore a good determinant of membrane area. A larger membrane surface area results in a larger membrane capacitance value. If PS1 (−/−) neurons were larger, then the membrane capacitance values would be expected to be larger for this population of neurons. However, we found no significant difference in the membrane capacitance values among the three populations [Fig. 1E; 10.1 ± 0.5 pF (n = 71) for PS1 (+/+) neurons vs. 9.9 ± 0.4 pF (n = 94) for PS1 (−/−) neurons; P = NS; one-way ANOVA]. PS1 (+/−) neurons had a similar membrane capacitance value of 11.3 ± 0.7 pF (n = 28). To further ensure that our findings were not influenced by cell size variations, we normalized our peak current data by cell size using individual cell capacitance measures to determine peak current density (pA/pF). As shown in Fig. 1F, peak current density was significantly different across the three groups (one-way ANOVA, P = 0.00001). Peak current density was significantly larger in the PS1 (−/−) neurons (45.7 ± 2.7 pA/pF; n = 94) than in PS1 (+/+) control neurons (29.6 ± 2.0 pA/pF; n = 71; P < 0.005, Scheffé's test). After correction for cell size variation, the PS1 (+/−) neurons had an intermediate peak current density (36.3 ± 4.8 pA/pF; n = 28) again suggesting a gene dosage effect of PS1.

The voltage-dependent properties of the WC current appeared unaltered in the PS1 (−/−) neurons. We found no significant difference in the voltage dependence of activation among the three populations. The half-maximal activation voltage was −25.0 ± 0.6 mV (n = 71) for PS1 (+/+) neurons, −26.5 ± 0.5 mV (n = 94) for PS1 (−/−) neurons, and −25.7 ± 1.1 mV (n = 28) for PS1 (+/−) neurons (one-way ANOVA, P = N.S.). Slope factors were also similar among the three groups [5.5 ± 0.2 mV for PS1 (+/+) neurons, 5.4 ± 0.2 mV for PS1 (−/−) neurons and 6.1 ± 0.4 mV for PS1 (+/−) neurons, one-way ANOVA, P = NS].

We next attempted to determine whether the current density of particular classes of HVA Ca^{2+} channels is increased in the PS1 (−/−) neurons. Pharmacological studies have identified 5 types of HVA channels in central neurons. These include N-, L-, P-, Q-, and R-type channels (Tsien et al. 1991), all of which appear to represent distinct gene families and are expressed to various degrees in cortical neurons in this age range (Randall and Tsien 1995; Snutch et al. 1990, 1991; Snutch and Reiner 1992; Zhang et al. 1993). Class C and D genes encode L-type channel α1 subunits with high affinity for dihydropyridine Ca^{2+} channel antagonists. The class B gene encodes N-type channels with high affinity for ω-conotoxin GVIA. The class A gene encodes P- and Q-type channels. P-type channels are sensitive to low concentrations of ω-agatoxin IVA while Q-type currents can be isolated based on their sensitivity to ω-conotoxin MVIIC once N- and P-type currents have been blocked. Class E channels have features of an R-type channel that is resistant to block by known Ca^{2+} channel blockers except Cd^{2+}. The contributions of the various HVA Ca^{2+} channel subtypes (N, L, P, Q, and R) can therefore be determined by toxin sensitivity and current subtraction. R-type channels are resistant to all known Ca^{2+} channel blockers, therefore the contribution of R-type currents was defined as any current remaining in the presence of blockers for all the other channel subtypes.

One or more of these channel blockers were applied sequentially to each cell in the following order: nifedipine (5 μM), ω-conotoxin GVIA (1 μM), ω-agatoxin IVA (100 nM) and ω-conotoxin MVIIC (2 μM). We were able to apply all four blockers in some but not every cell, so the n-values vary for each blocker. L-type current was defined as the component of the WC current that was sensitive to block by 5 μM nifedipine. N-type current was defined as the component of the remaining WC current sensitive to block by 1 μM ω-conotoxin GVIA. P-type current was defined as the component of the remaining

WC current sensitive to block by 100 nM ω-agatoxin IVA. Q-type current was defined as the component of the remaining WC current sensitive to block by 2 μM ω-conotoxin MVIIC. Because N- and P-type currents were already blocked, the effects of ω-conotoxin MVIIC on those current types did not confound our data. MVIIC-sensitive currents were only assessed in cells where ω-conotoxin GVIA and ω-agatoxin IVA were already applied. R-type current was defined as the component of the current remaining in the presence of all four blockers. Each blocker was applied and the peak current amplitude was allowed to stabilize for 2–4 min prior to data acquisition. Peak current was monitored periodically during drug application by a ramp voltage protocol from –110 to +50 mV at 0.5 mV/ms. After stabilization of the peak current amplitude in the drug solution, data acquisition began. The next blocker was then added and the current was allowed to stabilize again prior to data acquisition. In control cells, current rundown was typically <10% and followed a linear progression during an experiment of similar duration using identical voltage protocols.

We first tested whether the increase in total current involved a specific increase in L-type current by examining the size of the nifedipine-sensitive current. If the percentage of the WC current carried by L-type Ca^{2+} channels is increased in the PS1-deficient neurons, the percentage of the current blocked by the dihydropyridine, nifedipine (5 μM) should be increased in these neurons as well. As shown in Fig. 2, A–D, our pharmacological analysis supported this hypothesis and demonstrated that PS1 ($-/-$) neurons were more sensitive to block by 5 μM nifedipine, suggesting a specific increase in L-type Ca^{2+} current amplitude. For PS1 ($+/+$) neurons, the percentage of the WC current blocked by nifedipine was 33.8 ± 2.5% ($n = 31$) compared with 44.4 ± 2.4% ($n = 37$; $P = 0.003$, Student's t-test) for PS1 ($-/-$) neurons (Fig. 2C). A similar result was obtained when the total current blocked by nifedipine was analyzed. For PS1 ($+/+$) neuron, the total current blocked by nifedipine was 101.8 ± 9.2 pA ($n = 31$) compared with 165.8 ± 15.1 pA for PS1 ($-/-$) neurons ($n = 37$; $P = 0.001$, Student's t-test).

To address the possibility that HVA Ca^{2+} channel subtypes in addition to L-type contribute to the phenotype of increased WC HVA Ca^{2+} current in PS1-deficient neurons, we conducted pharmacological experiments designed to isolate P-, N-, Q-, and R-type channels as described in the preceding text. Using the P-type specific Ca^{2+} channel blocker, ω-agatoxin IVA (100 nM), we found that the percentage of the WC current carried by P-type Ca^{2+} channels is increased in the PS1-deficient neurons as well. As shown in Fig. 2, E and F, the
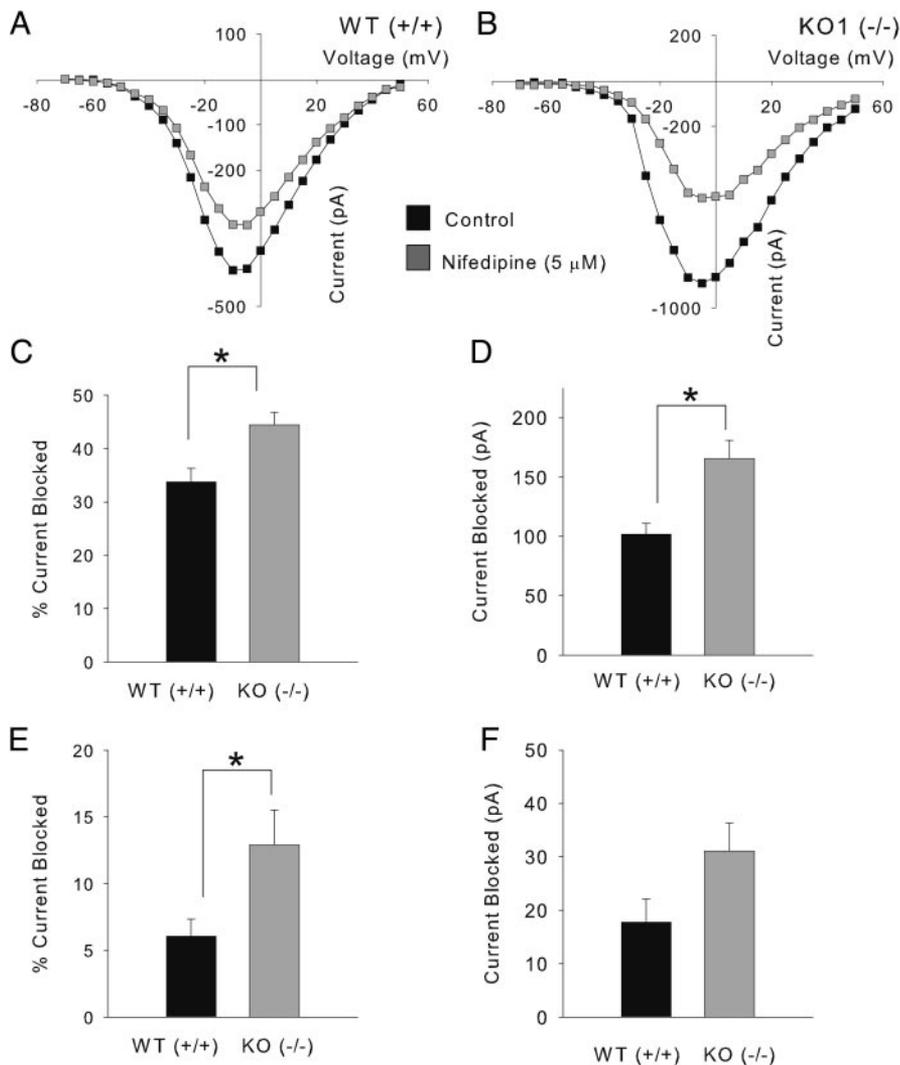

FIG. 2. L- and P-type Ca^{2+} channel activity is specifically upregulated in PS1 ($-/-$) neurons. A: plot of peak current vs. test pulse voltage under control conditions (■) and in the presence of 5 μM nifedipine (■) for a representative PS1 WT ($+/+$) neuron. B: plot of peak current versus test pulse voltage under control conditions (■) and in the presence of 5 μM nifedipine (■) for a representative PS1 ($-/-$) neuron. C and D: bar graphs depicting a statistical summary of the percentage of the whole cell current (C) and the total pA of whole cell current (D) that was blocked by 5 μM nifedipine for populations of PS1 WT ($+/+$) ($n = 31$) and PS1 ($-/-$) neurons ($n = 37$). E and F: bar graphs depicting a statistical summary of the percentage of the whole cell current (E) and the total pA of whole cell current (F) that was blocked by 100 nM ω-agatoxin IVA for populations of PS1 WT ($+/+$) neurons ($n = 14$) and PS1 ($-/-$) neurons ($n = 14$). Error bars depict SE. *, statistically significant differences of $P < 0.05$ as determined Student's t-test. NS, statistical nonsignificance.

TABLE 1. *Contributions of L-, N-, P-, Q- and R-type Ca^{2+} channels to the whole cell current*

Channel Subtype	Percentage Current Blocked			Total pA Current Blocked		
	WT	PS1-KO	P	WT	PS1-KO	P
Nifedipine Sensitive (L)	33.8 ± 2.5	44.4 ± 2.4	0.003	101.8 ± 9.2	165.8 ± 15.1	0.001
n	31	37	*	31	37	*
ω-conotoxin GVIA Sensitive (N)	27.3 ± 5.4	21.5 ± 3.3	P = N.S.	89.3 ± 21.2	75.9 ± 26.1	P = N.S.
n	10	10		14	14	
ω-agatoxin IVA Sensitive (P)	6.1 ± 1.3	12.9 ± 2.6	P = .02	17.8 ± 4.3	31.1 ± 5.3	P = .07
n	14	9	*	14	9	
ω-conotoxin MVIIC Sensitive (Q)	10.9 ± 5.0	10.7 ± 5.0	P = N.S.	30.4 ± 15.0	62.7 ± 48.5	P = N.S.
n	13	8		13	8	
Toxin Insensitive (R)	39.6 ± 7.9	33.6 ± 5.8	P = N.S.	130.6 ± 39.5	88.9 ± 25.2	P = N.S.
n	7	5		7	5	

Values are presented as means ± SE; (n, number of cells). Statistically significant differences were determined using Student's t-test with P values as indicated. NS denotes statistical nonsignificance. Drugs were applied sequentially in the order indicated at the following concentrations: nifedipine (5 μM), ω-conotoxin GVIA (1 μM), ω-agatoxin IVA (100 nM), ω-conotoxin MVIIC (2 μM). *P ≤ 0.05.

component of the WC current blocked by ω-agatoxin IVA (100 nM) was greater in PS1 (−/−) neurons compared with wild-type neurons (6.1 ± 1.3%; $n = 14$ vs. 12.9 ± 2.6%; $n = 9$; $P = 0.02$, Student's t-test). A similar trend was obtained when the total current blocked by ω-agatoxin IVA was analyzed. For PS1 (+/+) neuron, the total current blocked by ω-agatoxin IVA was 17.8 ± 4.3 pA ($n = 14$) compared with 31.1 ± 5.3 pA for PS1 (−/−) neurons ($n = 9$; $P = 0.07$, Student's t-test).

Using the additional specific Ca^{2+} channel blockers, ω-conotoxin GVIA (1 μM; N-type) and ω-conotoxin MVIIC (2 μM; Q-type), we found no significant changes in the amplitudes of N- or Q-type channels as summarized in Table 1. The contribution of R-type or resistant channels was also unchanged.

Because PS1-deficiency (−/−) significantly impairs intracellular Ca^{2+} homeostasis (Leissring et al. 2002; Yang and Cook 2004; Yoo et al. 2000), we were interested in the relationship between decreased intracellular Ca^{2+} stores and the observed alterations in Ca^{2+} current amplitude. Therefore we repeated these experiments under several conditions in which intracellular Ca^{2+} levels could be experimentally manipulated. In the first set of experiments, we repeated the original experiment described in Fig. 1 in the presence of 10 mM intracellular BAPTA. This concentration of BAPTA is sufficient to buffer any intracellular Ca^{2+} signal. If the observed increase in Ca^{2+} current amplitude is related to PS1-dependent impairment of intracellular Ca^{2+} signaling, then we predicted that WT PS1 (+/+) neurons recorded in the presence of 10 mM BAPTA would have a WC Ca^{2+} current phenotype that was similar to untreated PS1 (−/−) neurons. We further predicted there would be no effect of this experimental manip-

ulation on the PS1-deficient neurons because the intracellular Ca^{2+} level was already reduced in these neurons. As shown in Fig. 3, this was indeed the case. WT PS1 (+/+) neurons dialyzed with 10 mM BAPTA had peak Ca^{2+} current amplitude that is significantly larger relative to untreated WT PS1 (+/+) neurons (472.7 ± 45.8 pA; $n = 22$ vs. 270.7 ± 16.5 pA; $n = 71$; $P < 0.005$, Scheffé's test; Fig. 3A). Chelation of intracellular Ca^{2+} with BAPTA produced an increase in Ca^{2+} current amplitude that was comparable to the increase caused by PS1-deficiency (Fig. 3A). By contrast, there was no effect of 10 mM BAPTA on peak current amplitude in the PS1 (−/−) population (Fig. 3A, $P = $ N.S., Scheffé's test). Average peak current density in the BAPTA-treated WT PS1 (+/+) neurons was also significantly larger relative to untreated WT PS1 (+/+) neurons (52.4 ± 4.4 pA/pF; $n = 22$ versus 29.6 ± 2.0 pA/pF; $n = 71$; $P < 0.005$, Scheffé's test; Fig. 3C). There was no effect of 10 mM BAPTA on peak current density in the PS1 (−/−) population (Fig. 3C, $P = $ NS, Scheffe' test).

The use of caffeine offers another well-established experimental manipulation to alter intracellular Ca^{2+} homeostasis, and we tested whether the effects of caffeine were different in the PS-1 deficient mice. To test this idea, we chronically exposed WT PS1 (+/+) neurons to 500 μM caffeine for 10–12 h prior to the electrophysiology experiment. Caffeine exposure was maintained during the electrophysiology experiment by the inclusion of 500 μM caffeine in the background solution and the external recording solution. This treatment should result in the chronic depletion of Ca^{2+} from intracellular stores. Again, if the observed increase in Ca^{2+} current amplitude is related to PS1-dependent impairment in intracel-
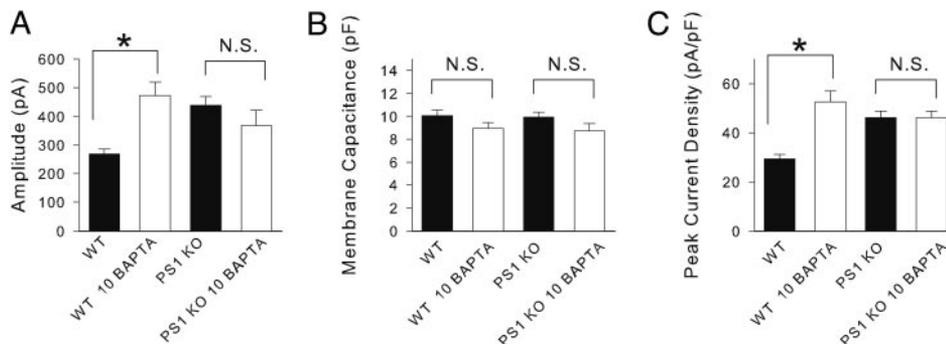

FIG. 3. Dialysis with 10 mM 1,2-bis-(o-aminophenoxy)ethane-N,N,N′,N′-tetraacetic acid produces a PS1 (−/−)-like Ca^{2+} current phenotype in PS1 WT (+/+) neurons. A–C: bar graphs depicting a statistical summary of the peak current amplitude (A), the membrane capacitance (B), and the peak current density (C) for populations of PS1 WT (+/+) neurons ($n = 94$), PS1 WT (+/+) neurons treated with 10 mM BAPTA ($n = 22$), PS1 (−/−) neurons ($n = 71$), and PS1 (−/−) neurons treated with 10 mM BAPTA ($n = 16$). Error bars depict SE. *, statistically significant differences of $P < 0.005$ as determined by one-way ANOVA followed by post hoc Scheffé's analysis. NS, statistical nonsignificance.

lular Ca^{2+} signaling, then we predicted that WT PS1 ($+/+$) neurons that have been chronically exposed to caffeine should have a WC Ca^{2+} current phenotype that is similar to PS1 ($-/-$) neurons. As shown in Fig. 4, this was indeed the case. WT PS1 ($+/+$) neurons that were been chronically exposed to 500 μM caffeine had a peak current amplitude that was significantly larger relative to untreated WT PS1 ($+/+$) neurons (434.4 ± 55.7 pA; $n = 23$ vs. 270.7 ± 16.5 pA; $n = 71$; $P < 0.005$, Scheffé's test; Fig. 4A. Chronic caffeine exposure produced an increase in Ca^{2+} current amplitude that was comparable to the increase caused by PS1-deficiency (Fig. 4A). By contrast, there was no effect of caffeine treatment on peak current amplitude in the PS1 ($-/-$) population (Fig. 4A, $P =$ NS, Scheffé's test). Average peak current density in the caffeine-treated WT PS1 ($+/+$) neurons was also significantly larger relative to untreated WT PS1 ($+/+$) neurons (41.7 ± 4.5 pA/pF; $n = 23$ vs. 29.6 ± 2.0 pA/pF; $n = 71$; $P < 0.005$, Scheffe' test; Fig. 4B). There was no effect of caffeine treatment on peak current density in the PS1 ($-/-$) population (Fig. 4B, $P =$ NS, Scheffé's test). More specifically, the magnitude of L-type Ca^{2+} current was increased in the caffeine-treated PS1 WT ($+/+$) neurons to a level similar to that observed for the untreated PS1 ($-/-$) neurons as shown in Fig. 5. We observed no effect of chronic caffeine exposure on the magnitude of the L-type Ca^{2+} current in the PS1 ($-/-$) neurons (Fig. 5).

DISCUSSION

Our results provide strong evidence suggesting that PS1 deficiency alters the activity of L- and P-type Ca^{2+} channels in mouse cortical neurons. Peak Ca^{2+} current amplitude and peak current density was increased in cortical neurons in the absence of PS1. The increase in Ca^{2+} channel activity appeared to be mediated by a selective increase in Ca^{2+} flux mediated by dihydropyridine-sensitive L-type Ca^{2+} channels and a smaller increase in ω-Agatoxin IVA-sensitive P-type Ca^{2+} channels. These findings suggest that PS1 regulates neuronal intracellular Ca^{2+} homeostasis by influencing calcium signaling from both intracellular and extracellular sources.

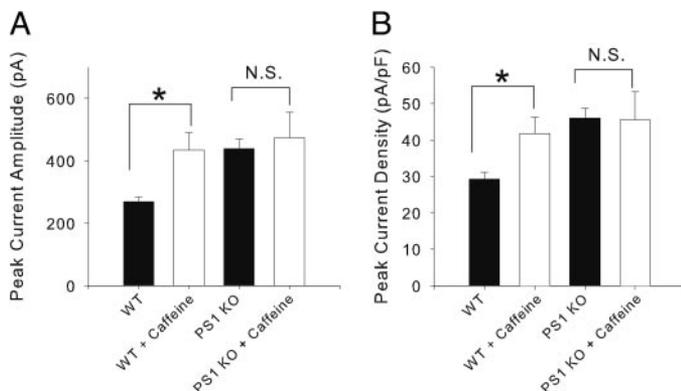FIG. 5. Chronic exposure to caffeine increases L-type channel activity in PS1 WT ($+/+$) neurons. Bar graph depicting a statistical summary of the percentage current block by 5 μM nifedipine for populations of PS1 WT ($+/+$) neurons ($n = 11$), PS1 WT ($+/+$) neurons treated with caffeine ($n = 10$), PS1 ($-/-$) neurons ($n = 16$) and PS1 ($-/-$) neurons treated with caffeine ($n = 8$). Error bars depict SE. *, statistically significant differences of $P < 0.01$ as determined by one-way ANOVA followed by post hoc Scheffé's analysis. NS, statistical nonsignificance.
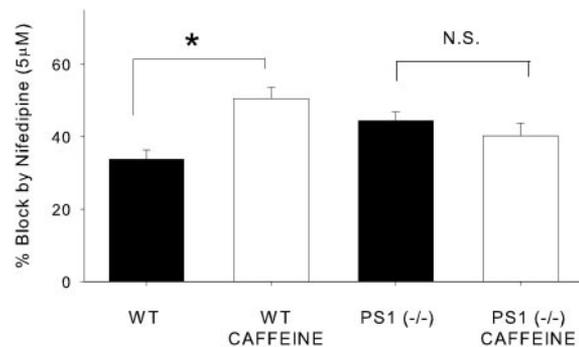
Potential mechanisms for the upregulation of L- and P-type Ca^{2+} channel activity

The mechanism by which PS1-deficiency increases Ca^{2+} channel activity in cultured cortical neurons is not clear, but our data allow us to speculate on several potential mechanisms. First, it has been recently reported that the β-subunit of the voltage-gated Na^+ channel is a target for PS1/γ-secretase-dependent cleavage (Kim et al. 2005; Wong et al. 2005). Although PS1-dependent cleavage of a Ca^{2+} channel subunit has not yet been reported in the literature, it is possible that one or more of the subunits comprising the L- and P-type Ca^{2+} channels may be substrates for PS1-dependent cleavage resulting in alterations in channel function. It has been reported that neuronal class C L-type Ca^{2+} channels are proteolytically cleaved by calpain resulting in full-length and short isoforms with different functional properties (Hell et al. 1993, 1996; Klöckner et al. 1995; Wei et al. 1994). The full-length isoform gives rise to a channel with four- to sixfold lower conductance than the short form, which is truncated at the C terminus (Klöckner et al. 1995; Wei et al. 1994). It is conceivable that PS1 might similarly cleave the L-type Ca^{2+} channel in cortical neurons. However, if this was the case, one would expect the full-length form to be most abundant in PS1-deficient neurons, resulting in reduced peak current amplitude. However, peak Ca^{2+} current amplitude is increased in PS1-deficient neurons not decreased. Therefore it is unlikely that PS1-dependent cleavage of the channel protein can account for our findings.

Second, Ca^{2+} channel expression in the plasma membrane may be upregulated as a result of PS1 deficiency. This possibility cannot be ruled out based on our current data; however, the new channels would have to available in a pool near the plasma membrane, awaiting rapid insertion based on the data obtained in our recordings of WT neurons dialyzed with 10 mM BAPTA. In these experiments, Ca^{2+} current amplitude was increased to PS1 ($-/-$) levels within a time frame less than our 5-min dialysis period. This time frame would appear too rapid for the generation and insertion of new channel proteins but does not rule out a readily available pool of channels. Future experiments aim to address this issue more fully using immunohistochemistry and/or Western blotting approaches.

FIG. 4. Chronic exposure to caffeine produces a PS1 ($-/-$)-like Ca^{2+} current phenotype in PS1 WT ($+/+$) neurons. A and B: bar graphs depicting a statistical summary of the peak current amplitude (A) and the peak current density (B) for populations of PS1 WT ($+/+$) neurons ($n = 71$), PS1 WT ($+/+$) neurons treated with caffeine ($n = 23$), PS1 ($-/-$) neurons ($n = 94$), and PS1 ($-/-$) neurons treated with caffeine ($n = 12$). Error bars depict SE. *, statistically significant differences of $P < 0.005$ as determined by one-way ANOVA followed by post hoc Scheffé's analysis. NS, statistical nonsignificance.

Third, the PS1-dependent decrease in intracellular Ca^{2+} levels may alter the activity of voltage-gated plasma membrane Ca^{2+} channels. It is well established that intracellular Ca^{2+} plays a pivotal role in regulating a number of critical functions in the CNS including axonal outgrowth and targeting, learning and memory, neuronal excitation, and neurotransmitter release (Catterall 1999; Forscher 1989; Rizzuto 2001; Rose and Konnerth 2001). Ion channel activity is also regulated by intracellular Ca^{2+} signals. As a specific example, L-type Ca^{2+} channels are strongly inhibited following activation of a subset of muscarinic acetylcholine receptors coupled to phospholipase C (PLC) activation and subsequent release of IC Ca^{2+} from IP_3-sensitive stores (Howe and Surmeier 1995; Stewart et al. 1999). Therefore it is possible that the observed changes in Ca^{2+} channel activity may result from reduced intracellular Ca^{2+} signals in the PS1 ($-/-$) neurons. Our BAPTA and caffeine data would support this idea and suggest that PS1-dependent dysregulation of intracellular Ca^{2+} homeostasis is intimately related to the increase in peak current amplitude.

Finally, because PS1 effects a variety of other pathways including development, protein trafficking, apoptosis and neurogenesis, it must be considered that the effects of PS1 deficiency on voltage-gated Ca^{2+} channel activity may be via a much more indirect chain of events.

Functional significance of HVA Ca^{2+} channel regulation

HVA Ca^{2+} channels are the primary regulators of excitability and input integration at the cell soma and dendrites and contribute to neurotransmitter release at synapses in the CNS (Catterall 2000; Hille 2001; Meir et al. 1999). At the soma, voltage-gated L-type Ca^{2+} channels help to maintain longer-lasting depolarizations to reduce firing threshold and regulate repetitive firing as well as shaping regenerative action potentials. In addition, Ca^{2+} flux via L-type HVA Ca^{2+} channels localized at the soma has been show to regulate gene transcription (Finkbeiner and Greenberg 1998; Gallin and Greenberg 1995). Voltage-gated P-type Ca^{2+} channels initiate neurotransmission at fast synapses (Catterall et al. 2000). Under normal conditions, HVA Ca^{2+} channels, which mediate Ca^{2+} influx, are tightly regulated by a number of intracellular signal transduction mechanisms to ensure proper function of central neurons. These channels and the regulatory mechanisms that govern them are important determinants of neuronal activity. Based on the central role of voltage-gated Ca^{2+} channels in regulating neuronal excitability, synaptic potentials and neurotransmission, alterations in the physiological properties or neurotransmitter regulation of HVA Ca^{2+} channels in cortical neurons may have an enormous impact on cortical function. Thus our results suggest a novel means by which PS1 may significantly influence neuronal excitability and ultimately synaptic transmission.

Significance of PS1 in regulating calcium signaling

A growing number of studies argue that PS1 regulates intracellular Ca^{2+} signaling. Every FAD-related PS1/2 mutation that has been examined displays altered intracellular Ca^{2+} signaling (LaFerla 2002). Regarding PS1 FAD mutations, the data are consistent with the idea that Ca^{2+} levels in the endoplasmic reticulum (ER) are elevated (Begley et al. 1999;

Guo et al. 1996, 1999a,b; Herms et al. 2003; Leissring et al. 1999a, 2000, 2002; Parent et al. 1999; Schneider et al. 2001; Stutzmann et al. 2004; Yoo et al. 2000). Conversely, PS1 deficiency leads to lower Ca^{2+} levels in the ER (Leissring et al. 2002; Nakajima et al. 2001). PS2-deficient cells, by contrast, display no defect in intracellular Ca^{2+} homeostasis (Leissring et al. 2002). Importantly, new findings strongly suggest that APP metabolism may play a significant role in mediating the effects of PS1 on intracellular Ca^{2+} signaling. Gamma-secretase inhibitors, which block PS1 activity (Wolfe 2001), reduce both $A\beta$ production and ER Ca^{2+} stores. Also, APP deficiency appears to mimic the effects of PS1 deficiency on ER Ca^{2+} levels (Leissring et al. 2002). Thus on one hand, reduced intracellular Ca^{2+} levels are associated with reduced levels of $A\beta$, whereas on the other hand, evoking Ca^{2+} increases (Querfurth and Selkoe 1994) or increasing synaptic activity stimulates $A\beta$ production (Kamenetz et al. 2003). Do such findings suggest Ca^{2+} signaling controls PS1 activity and subsequently mediates APP metabolism? Conversely, does PS1 activity regulate Ca^{2+} signaling? Currently, there are no satisfactory answers to such questions.

A large literature uniformly supports the idea that intracellular calcium signaling is influenced by PS1 function (Begley et al. 1999; Guo et al. 1999a; Herms et al. 2003; Ito et al. 1994; LaFerla 2002; Leissring et al. 1999a, 1999b, 2002; Stutzmann et al. 2004; Yang and Cook 2004; Yoo et al. 2000) and has been validated using a wide variety of preparations including, *Xenopus* oocytes (Leissring et al. 1999b), fibroblasts (Leissring et al. 2002), neurons (Yang and Cook 2004; Yoo et al. 2000), and hippocampal slices (Herms et al. 2003). Overall the findings from different labs are quite concordant. Yet there are differences as well. For example, in slices intracellular stores have been reported to increase in PS1 KO neurons rather than decrease as observed by us (Yang and Cook 2004) and others (Yoo et al. 2000). Although it is possible such differences are due to methodological issues, a more interesting possibility arises from the implications of the data reported herein. Our findings show that PS1 deficiency increases the entry of calcium from extracellular sources. Yet we and others have also reported that PS1 deficiency reduces cytoplasmic calcium signals derived from intracellular calcium stores (Yang and Cook 2004; Yoo et al. 2000). We interpret these data to show that impaired intracellular calcium signaling leads to a compensatory increase in calcium entry mediated by voltage-gated calcium channels. It is quite likely that the compensatory action of voltage-gated calcium channels in PS1 KO neurons is attenuated in younger neuronal cultures where the expression of these channels is delayed. By waiting to carry out our experiments in more mature neurons, we were able observe the effects of PS1 deficiency on calcium channels, whereas in younger cultures, the effects of PS1 deficiency on ER calcium stores could be revealed with less apparent opposition from extracellular calcium sources. Thus it is possible that the intracellular calcium response observed in PS1 neuronal KO slices (Herms et al. 2003) were mediated by changes in the influx of calcium from extracellular sources.

Taken collectively, it appears PS1 activity and Ca^{2+} signaling interact in complex and, as yet, poorly understood ways. Based on the recent suggestion that $A\beta$ is associated with feedback inhibition of synaptic activity (Kamenetz et al. 2003), it is tempting to speculate that PS1 activity and the Ca^{2+}

signaling systems in neurons might participate in some form of dual feedback regulation. The observed effects of PS1 on voltage-gated Ca^{2+} channels could contribute to such feedback regulation.

Our data suggest that decreased intracellular calcium signaling induced by PS1 loss of function, in turn, increases voltage-dependent Ca^{2+} channel activity. Thus PS1 may influence intracellular Ca^{2+} homeostasis by counter-regulation of multiple components of the Ca^{2+} signaling system in neurons. This idea is consistent with other findings that nifedipine reduces H_2O_2-induced toxicity in PS1-deficient neurons (Nakajima et al. 2001). One possible functional consequence of such processes is that the normal activity of PS1 may limit the neurotoxicity mediated by HVA Ca^{2+} channels in response to a variety of toxic insults thought to be associated with multiple neurodegenerative disorders as well as aging.

REFERENCES

Baumeister R, Leimer U, Zweckbronner I, Jakubek C, Grunberg J, and Haass C. Human presenilin-1, but not familial Alzheimer's disease (FAD) mutants, facilitate *Caenorhabditis elegans* Notch signalling independently of proteolytic processing. *Genes Funct* 1: 149–159, 1997.

Begley JG, Duan W, Chan S, Duff K, and Mattson MP. Altered calcium homeostasis and mitochondrial dysfunction in cortical synaptic compartments of presenilin-1 mutant mice. *J Neurochem* 72: 1030–1039, 1999.

Cai D, Leem JY, Greenfield JP, Wang P, Wang R, Lopes KO, Kim SH, Zheng H, Greengard P, Sisodia SS, Thinakaran G, and Xu H. Presenilin-1 regulates intracellular trafficking and cell surface delivery of beta APP. *J Biol Chem* 278: 3446–3454, 2002.

Catterall WA. Interactions of presynaptic Ca^{2+} channels and snare proteins in neurotransmitter release. *Ann NY Acad Sci* 868:159, 1999.

Catterall WA. Structure and regulation of voltage-gated Ca^{2+} channels. *Annu Rev Cell Dev Biol* 16: 521–555, 2000.

Doan A, Thinakaran G, Borchelt DR, Slunt HH, Ratovitsky T, Podlisny M, Selkoe DJ, Seeger M, Gandy SE, Price DL, and Sisodia SS. Protein topology of presenilin 1. *Neuron* 17: 1023–1030, 1996.

Feng R, Rampon C, Tang YP, Shrom D, Jin J, Kyin M, Sopher B, Miller MW, Ware CB, Martin GM, Kim SH, Langdon RB, Sisodia SS, and Tsien JZ. Deficient neurogenesis in forebrain-specific presenilin-1 knockout mice is associated with reduced clearance of hippocampal memory traces. *Neuron* 32: 911–926, 2001.

Finkbeiner S and Greenberg ME. Ca^{2+} channel-regulated neuronal gene expression. *J Neurobiol* 37: 171–189, 1998.

Foehring RC and Lorenzon NM. Neuromodulation, development and synaptic plasticity. *Can J Exp Psychol* 53: 45–64, 1999.

Forscher P. Calcium and polyphosphoinositide control of cytoskeletal dynamics. *Trends Neurosci* 12: 468–474, 1989.

Gallin WJ and Greenberg ME. Calcium regulation of gene expression in neurons: The mode of entry matters. *Curr Opin Neurobiol* 5: 367–374, 1995.

Guo Q, Fu W, Sopher BL, Miller MW, Ware CB, Martin GM, and Mattson MP. Increased vulnerability of hippocampal neurons to excitotoxic necrosis in presenilin-1 mutant knock-in mice. *Nat Med* 5: 101–106, 1999a.

Guo Q, Furuakwa K, Sopher BL, Pham DG, Xie J, Robinson N, Martin GM, and Mattson MP. Alzheimer's PS-1 mutation perturbs calcium homeostasis and sensitizes PC12 cells to death induced by amyloid β-peptide. *Neuroreport* 8: 379–383, 1996.

Guo Q, Sebastion L, Sopher BL, Miller MW, Ware CB, Martin GM, and Mattson MP. Increased vulnerability of hippocampal neurons from prese-

nilin-1 mutant knock-in mice to amyloid beta-peptide toxicity: central roles of superoxide production and caspase activation. *J Neurochem* 72: 1019–1029, 1999b.

Haass C. Presenilins: genes for life and death. *Neuron* 18: 687–690, 1997.

Hell JW, Appleyard SM, Yokoyama CT, Warner C, and Catterall WA. Differential phosphorylation of two size forms of the N-type calcium channel α1 subunit which have different COOH termini. *J Biol Chem* 269: 7390–7396, 1994.

Hell JW, Westenbroek RE, Breeze LJ, Wang KK, Chavkin C, and Catterall WA. N-Methyl-D-aspartate receptor-induced proteolytic conversion of postsynaptic class C L-type calcium channels in hippocampal neurons. *Proc Natl Acad Sci USA* 93: 3362–3367, 1996.

Hell JW, Westenbroek RE, Warner C, Ahlijanian MK, Prystay WGMM, Snutch TP, and Catterall WA. Identification and differential subcellular localization of the neuronal class C and class D, L-type calcium channel alpha 1 subunits. *J Biol Chem* 123: 949–962, 1993.

Herms J, Schneider I, Dewachter I, Caluwaerts N, Kretzschmar HA, and Van Leuven F. Capacitative calcium entry is directly attenuated by mutant presenilin-1, independent of the expression of the amyloid precursor protein. *J Biol Chem* 278: 2484–2489, 2003.

Hille, B. *Ion Channels of Excitable Membranes.* Sinauer Associates. 2001.

Howe AR and Surmeier DJ. Muscarinic receptors modulate N-, P-, and L-type calcium currents in rat striatal neurons through parallel pathways. *J Neurosci* 15: 458–469, 1995.

Ikeuchi T and Sisodia SS. The notch ligands, Delta1 and Jagged2, are substrates for presenilin-dependent "gamma-secretase" cleavage. *J Biol Chem* 278: 7751–7754, 2003.

Ito E, Oka K, Etcheberrigaray R, Nelson TJ, McPhie DL, Tofel-Grehl B, Gibson GE, and Alkon DL. Internal Ca^{2+} mobilization is altered in fibroblasts from patients with Alzheimer's disease. *Proc Natl Acad Sci USA* 91: 534–538, 1994.

Kamenetz F, Tomita T, Hsieh H, Seabrook G, Borchelt DR, Iwatsubo T, Sisodia SS, and Malinow R. APP processing and synaptic function. *Neuron* 37: 925–937, 2003.

Kim DY, MacKenzie Ingano LA, Carey BW, Pettingell WH, and Kovacs DM. Presenilin/γ-secretase-mediated cleavage of the voltage-gated sodium channel β2-subunit regulates cell adhesion and migration. *J Biol Chem* 280: 23251–23261, 2005.

Klöckner U, Mikala G, Varadi M, Varadi G, and Schwartz A. Involvement of the carboxyl-terminal region of the α1 subunit in voltage-dependent inactivation of cardiac calcium channels. *J Biol Chem* 270: 17306–17310, 1995.

LaFerla FM. Calcium dyshomeostasis and intracellular signalling in Alzheimer's Disease. *Nat Rev Neurosci* 3: 862–872, 2002.

Leem JY, Vijayan S, Han P, Cai D, Machura M, Lopes KO, Veselits ML, Xu H, and Thinakaran G. Presenilin 1 is required for maturation and cell surface accumulation of nicastrin. *J Biol Chem* 277: 19236–19240, 2002.

Leissring MA, Akbari Y, Fanger CM, Cahalan MD, Mattson MP, and LaFerla FM. Capacitative calcium entry deficits and elevated luminal calcium content in mutant presenilin-1 knockin mice. *J Cell Biol* 149: 793–797, 2000.

Leissring MA, Murphy MP, Mead TR, Akbari Y, Sugarman MC, Jannatipour M, Anliker B, Muller U, Saftig P, De Strooper B, Wolfe MS, Golde TE, and LaFerla FM. A physiologic signaling role for the gamma-secretase-derived intracellular fragment of APP. *Proc Natl Acad Sci USA* 99: 4697–4702, 2002.

Leissring MA, Parker I, and LaFerla FM. Presenilin-2 mutations modulate amplitude and kinetics of inositol 1,4,5-trisphosphate-mediated calcium signals. *J Biol Chem* 274: 32535–32538, 1999a.

Leissring MA, Paul BA, Parker I, Cotman CW, and LaFerla FM. Alzheimer's presenilin-1 mutation potentiates inositol 1,4,5-trisphosphate-mediated calcium signaling in *Xenopus* oocytes. *J Neurochem* 72: 1061–1068, 1999b.

Levitan D, Doyle TG, Brousseau D, Lee MK, Thinakaran G, Slunt HH, Sisodia SS, and Greenwald I. Assessment of normal and mutant human presenilin function in *Caenorhabditis elegans*. *Proc Natl Acad Sci USA* 93: 14940–14944, 1996.

Levy-Lahad E, Wasco W, Poorkaj P, Romano DM, Oshima J, Pettingell WH, Yu C, Jondro PD, Schmidt SD, Wang K, Crowley AC, Fu, Y.-H, Guenette SY, Galas D, Nemens E, Wijsman EM, Bird TD, Schellenberg GD, and Tanzi RE. Candidate gene for the chromosome 1 familial Alzheimer's disease locus. *Science* 269: 973–977, 1995.

Li X and Greenwald I. Membrane topology of the C. elegans SEL-12 presenilin. *Neuron* 17: 1015–1021, 1996.

Lorenzon NM and Foehring RC. Characterization of pharmacologically identified voltage-gated calcium channel currents in acutely isolated rat neocortical neurons. II. Postnatal development. *J Neurophysiol* 73: 1443–1451, 1995.

Marambaud P, Shioi J, Serban G, Georgakopoulos A, Sarner S, Nagy V, Baki L, Wen P, Efthimiopoulos S, Shao Z, Wisniewski T, and Robakis NK. A presenilin-1/gamma-secretase cleavage releases the E-cadherin intracellular domain and regulates disassembly of adherens junctions. *EMBO J* 21: 1948–1956, 2002.

Mattson MP, Guo Q, Furuakwa K, and Pederson WA. Presenilins, the endoplasmic reticulum, and neuronal apoptosis in Alzheimer's Disease. *J Neurochem* 70: 1–14, 1998.

May P, Reddy YK, and Herz J. Proteolytic processing of low density lipoprotein receptor-related protein mediates regulated release of its intracellular domain. *J Biol Chem* 277: 18736–18743, 2002.

Meir A, Ginsburg S, Butkevich A, Kachalsky SG, Kaiserman I, Ahdut R, Demirgoren S, and Rahamimoff R. Ion channels in presynaptic nerve terminals and control of transmitter release. *Physiol Rev* 79: 1019–1088, 1999.

Nakajima M, Miura M, Aosaki T, and Shirasawa T. Deficiency of presenilin-1 increases calcium-dependent vulnerability of neurons to oxidative stress in vitro. *J Neurochem* 78: 807–814, 2001.

Naruse S, Thinakaran G, Luo JJ, Kusiak JW, Tomita T, Iwatsubo T, Qian X, Ginty DD, Price DL, Borchelt DR, Wong PC, and Sisodia SS. Effects of PS1 deficiency on membrane protein trafficking in neurons. *Neuron* 21: 1213–1221, 1998.

Ni CY, Murphy MP, Golde TE, and Carpenter G. Gamma-secretase cleavage and nuclear localization of ErbB-4 receptor tyrosine kinase. *Science* 294: 2179–2181, 2001.

Parent A, Linden DJ, Sisodia SS, and Borchelt DR. Synaptic transmission and hippocampal long-term potential in transgenic mice expressing FAD-linked presenilin 1. *Neurobiol Dis* 6: 56–62, 1999.

Querfurth HW and Selkoe DJ. Calcium ionophore increases amyloid β peptide production by cultured cells. *Biochemistry* 33: 4550–4561, 1994.

Randall A and Tsien RW. Pharmacological dissection of of multiple types of Ca^{2+} channel currents in rat cerebellar granule neurons. *J Neurosci* 15: 2995–3012, 1995.

Rizzuto R. Intracellular Ca^{2+} pools in neuronal signalling. *Curr Opin Neurobiol* 11: 306–311, 2001.

Rogaev EI, Sherrington E, Levesque G, Ikeda, M, and St. George-Hyslop, P. Familial Alzheimer's disease in kindreds with missense mutations in a gene on chromosome 1 related to the Alzheimer's disease type 3 gene. *Nature* 376: 775–778, 1995.

Rose CR and Konnerth A. Stores not just for storage: intracellular calcium release and synaptic plasticity. *Neuron* 31: 519–522, 2001.

Schneider I, Reverse D, Dewachter I, Ris L, Caluwaerts N, Kuiperi C, Gilis M, Geerts H, Kretzschmar HA, Godaux E, Moechars D, Van Leuven F, and Herms JW. Mutant presenilins disturb neuronal calcium homeostasis in the brain of transgenic mice, decreasing the threshold for excitotoxicity and facilitating long-term potentiation. *J Biol Chem* 276: 11539–11544, 2001.

Selkoe DJ. Alzheimer's disease: genotypes, phenotypes and treatments. *Science* 275: 630–631, 1997.

Shen J, Bronson RT, Chen DF, Xia W, Selkoe DJ, and Tonegawa S. Skeletal and CNS defects in presenilin-1 deficient mice. *Cell* 89: 629–639, 1997.

Sherrington R, Rogaev EI, Liang Y, Rogaeva EA, Levesque G, Ikeda M, Chi H, Lin C, Li G, Holman K, Tsuda T, Mar L, Foncin, J.-F, Bruni AC, Montesi MP, Sorbi S, Rainero I, Pinessi L, Nee L, Chumakov I, Pollen D, Brookes A, Sanseau P, Polinsky RJ, Wasco W, Silva HARD, Haines JL, Pericak-Vance MA, Tanzi RE, Roses AD, Fraser PE, Romens JM, and George-Hyslop PHS. Cloning of a gene bearing missense mutations in early-onset familial Alzheimer's disease. *Nature* 375: 754–760, 1995.

Snutch TP, Leonard JP, Gilbert MM, Lester HA, and Davidson N. Rat brain expresses a heterogeneous family of Ca^{2+} channels. *Proc Natl Acad Sci USA* 87: 3391–3395, 1990.

Snutch TP and Reiner PB. Ca^{2+} channels: diversity of form and function. *Curr Opin Neurobiol* 2: 247–253, 1992.

Snutch TP, Tomlinson WJ, Leonard JP, and Gilbert MM. Distinct Ca^{2+} channels are generated by alternative splicing and are differentially expressed in the mammalian CNS. *Neuron* 7: 45–57, 1991.

Stewart AE, Yan Z, Sumeier DJ, and Foehring RC. Muscarine modulates Ca^{2+} channel currents in rat sensorimotor pyramidal cells via two distinct pathways. *J Neurophysiol* 81: 72–84, 1999.

Struhl G and Greenwald I. Presenilin is required for activity and nuclear access of Notch in *Drosophila*. *Nature* 398: 522–525, 1999.

Stutzmann GE, Caccamo A, LaFerla FM, and Parker I. Dysregulated IP$_3$ signaling in cortical neurons of knock-in mice expressing an Alzheimer's-linked mutation in Presenilin1 results in exaggerated Ca^{2+} signals and altered membrane excitability. *J Neurosci* 24: 508–513, 2004.

Surmeier DJ, Eberwine J, Wilson CJ, Stefani A, and Kitai ST. Dopamine receptor subtypes co-localize in rat striatonigral neurons. *Proc Natl Acad Sci USA* 89: 10178–10182, 1992.

Tsien RW, Ellinor PT, and Horne WA. Molecular diversity of voltage-dependent Ca^{2+} channels. *Trends Pharmacol Sci* 12: 349–354, 1991.

Wei X, Neely A, Lacerda AE, Olcese R, Stefani E, Perez-Reyes E, and Birnbaumer L. Modification of Ca^{2+} channel activity by deletions at the carboxyl terminus of the cardiac $\alpha 1$ subunit. *J Biol Chem* 269: 1635–1640, 1994.

Wolfe MS. Gamma-secretase inhibitors as molecular probes of presenilin function. *J Mol Neurosci* 17: 199–204, 2001.

Wolozin B, Alexander P, and Palacino J. Regulation of apoptosis by presenilin 1. *Neurobiol Aging* 19: S23–27, 1998.

Wong, H-K, Sakurai T, Oyama F, Kaneko K, Wada K, Miyazaki H, Kurosawa M, De Strooper B, Saftig P, and Nukina N. β-subunits of voltage-gated sodium channels are novel substrates of β-site amyloid precursor protein –cleaving enzyme (BACE1) and γ-secretase. *J Biol Chem* 280: 23009–23017, 2005.

Yang Y and Cook DG. Presenilin-1 deficiency impairs glutamate-evoked intracellular calcium responses in neurons. *Neuroscience* 124: 501–505, 2004.

Yoo AS, Cheng I, Chung S, Grenfell TZ, Lee H, Pack-Chung E, Handler M, Shen J, Xiz W, Tesco G, Saunders AJ, Ding K, Frosch MP, Tanzi RE, and Kim, T.-W. Presenilin-mediated modulation of capacitative calcium entry. *Neuron* 27: 561–572, 2000.

Zhang, J.-F, Randall AD, Ellinor PT, Horne WA, Sather WA, Tanabe T, Schwartz TL, and Tsien RW. Distinctive pharmacology and kinetics of cloned neuronal Ca^{2+} channels and their possible counterparts in mammalian CNS neurons. *Neuropharmacology* 32: 1075–1088, 1993.